H-mode edge current density profiles and scaling at ASDEX Upgrade

M.G. Dunne[1], A. Burckhart[2], P.A. Schneider[2], P.J. McCarthy[1], E. Wolfrum[2], R. Fischer[2], L. Giannone[2], K. Lackner[2], ASDEX Upgrade Team[2]

[1]*Department of Physics, University College Cork, Association Euratom-DCU, Cork, Ireland*

[2]*Max-Planck-Institut für Plasmaphysik, EURATOM Association, D-85748 Garching, Germany*

The most tested theory to describe Edge Localised Modes (ELMs) is the peeling-ballooning theory. This linear MHD theory predicts a critical edge pressure gradient and current density. Above these critical values unstable mode growth occurs, leading to an ELM crash. Observations of the critical pedestal pressure parameters have been made at several tokamaks [1, 2], all leading to the conclusion that the edge electron pressure gradient saturates before the ELM crash occurs; in some cases the gradient may remain saturated for several milliseconds. In other cases the ELM occurs just as the gradient reaches this value. The main unknown in all of these situations is the current density in the pedestal and its behaviour prior to an ELM crash.

Current density measurements in a tokamak rely mainly on determining the pitch angle of the magnetic field[3]; the confined plasma region is inaccessible to internal probes due to the high heat loads they would experience. However, the edge poloidal magnetic field in a medium sized tokamaks, such as ASDEX Upgrade, changes only slightly with the growth of a large edge current density, and the resulting small variations of pitch angle are challenging to measure.

However, there exists an alternative method of determining the edge current density. Through the use of an equilibrium solver the current density is obtained directly from the solution of the Grad-Shafranov equation. It was shown in [4] that, for an x-point plasma, moments of the current density distribution in the edge region can be recovered using only standard magnetic data. The examples shown in [4] are based on the geometry of ASDEX Upgrade, from which the data considered in this paper is also taken.

While the integrated edge current can be recovered, moments of the pressure profile cannot; only the total beta can be recovered from the magnetic data alone. However, once a pressure profile is experimentally determined it can then be used as a constraint for the CLISTE equilibrium solver. This, in combination with the magnetic measurements, now allows a shape and integrated value of the edge current density to be interpreted. In addition, the current in the scrape off layer (SOL) can also be constrained via shunt measurements of the poloidal current, providing a valuable extra constraint on the current density distribution. CLISTE fits these measurements by comparing the latest prediction for the measurements from a solution of the Grad-Shafranov equation. This is a combination of two source profiles, one being the pressure gradient and the other being related to the poloidal current, described by a curvature regularised cubic spline with, in the cases here, 11 knots. The final result is a minimisation of all residuals coupled with a pre-determined convergence criterion for the flux grid.

An example of this is shown in figure 1 for three timepoints from ASDEX Upgrade discharge #23223 in which a Neutral Beam Injection (NBI) power scan was performed. The electron pressure profiles were created by applying modified hyperbolic tangent (mtanh)

fits to data from ECE and Thomson Scattering diagnostics (electron temperature) and Lithium beam, DCN interferometer, and Thomson scattering diagnostics (electron density). The ion temperature was assumed to be equal to the electron temperature, and the ion density was diluted from the electron density according to a Z_{eff} of 1.9. The Thomson scattering data was used to align the temperature and density profiles.

As the applied power is increased, along with a density variation, the pedestal top pressure increases (figure 1(a). The pedestal width also increases (though the effect is small for the final power step), becoming dominated more by the electron temperature pedestal width. The peak edge gradient also increases, driving a larger amount of current (via bootstrap and Pfirsch-Schlüter mechanisms), as shown in figure 1(b). The ELM frequency in these time intervals changes from 125 ± 45Hz (red) to 100 ± 22Hz (blue) and finally to 105 ± 22Hz (black).

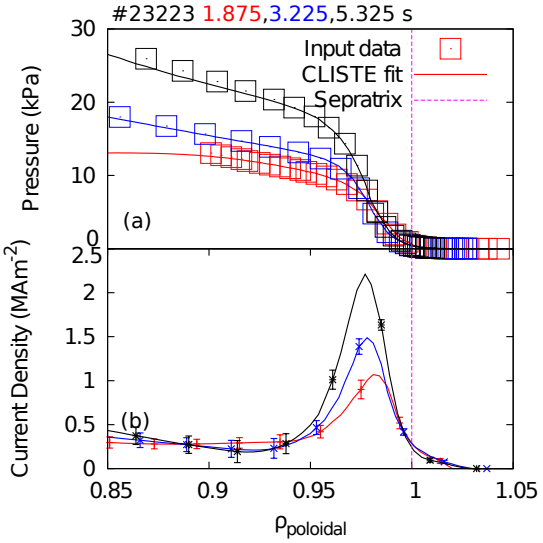

Figure 1: Current density from discharge #23223 with 5 MW (red), 7.5 MW (blue), and 10 MW (black) NBI heating. The boxes in (a) show the input pressure data. The error bars in (b) indicate the one sigma confidence bands

In order to asses the validity of the fits, as well as to determine the ability of magnetic and kinetic data to return a unique current density profile, the pressure profile from the high power phase of discharge #23223 was varied. First, the pressure profile was shifted radially in increments of 2 mm. Second, the parameters of the mtanh fits were varied to give a steeper (narrower) or shallower (wider) pedestal gradient (profile). The sensitivity of external magnetic measurements to changes in the current density distribution could be determined with these two methods. The influence of these changes to the pressure profiles on the fitting errors of the normal ($d\Psi$) and tangential (B_{theta}) components of the poloidal magnetic field is shown in figure 2.

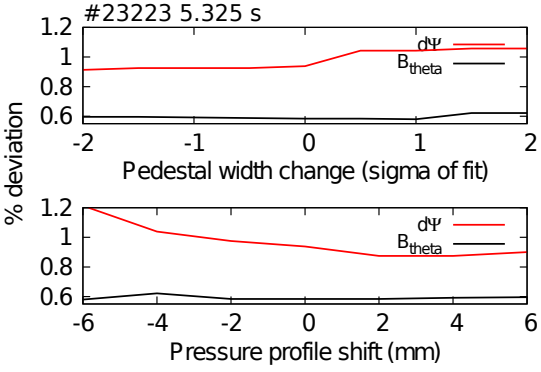

Figure 2: % fitting errors from normal (red) and tangential (black) magnetic measurements in pedestal width (a) and position scans (b) from discharge 23223 (NBI heating = 10 MW).

There is a well defined region in which the magnetic errors converge, indicating that this is the optimal region of parameter space for the pressure profile location and gradient. The x axis in (a) indicates the change to the pedestal width in terms of the confidence bands of the original tanh fit; -1 sigma means the narrowest possible fit with the allowed fitting parameters. The x axis in (b) denotes the shift of the pressure profile; 0 indicates a pressure profile with a separatrix temperature of 100 eV. Minimising the errors gives a peak gradient location with an error of ±2mm, outside of which the errors in the magnetic signals increase. The pedestal width (and hence peak gradient) cannot be determined with such high accuracy from magnetic data alone (though there seems

to be a maximum width, below which the normal field error increases sharply). These findings indicate that the reconstruction of a unique (and accurate) current density profile is indeed possible using the combination of external magnetic and internal pressure data.

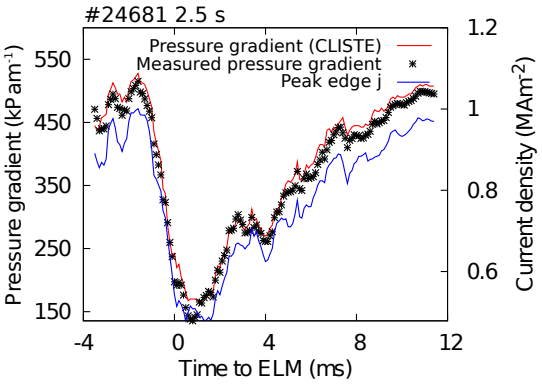

Figure 3: Time trace of peak pressure gradient from CLISTE (red) and from the input data (black points) and peak edge current density (blue) for ELM sycnhronised discharge #24681.

Determination of pre-ELM current density profiles is only one facet of analysis allowed by this method. Since several diagnostics with high time resolution ([5] and references therein) are combined and synchronised to a single ELM it is possible to obtain a picture of the current density evolution over an ELM cycle with high time resolution. Shown in figure 3 are the peak pressure gradient and peak edge current density timetraces for ASDEX Upgrade discharge #24681. In the pre-ELM phase the pressure gradient remains at a constant level and fluctuates leading up to the ELM crash, indicating that it is not a steady growth which eventually causes the ELM. It has been thought that, for such a time evolution, a delayed current density could be responsible for the eventual ELM crash.

It can clearly be seen in figure 3 that this is not the case and that the current density fluctuates in the same manner as the pressure gradient, as was also reported in [5]. Another interesting feature of the current density evolution in this case is the absence of a resistive delay in the current density evolution relative to the pressure gradient. This lack of delay can be accounted for by the recovery of the plasma volume after the ELM crash, also reported in [5].

Since the current density is made up of several separate drives, a complete study would investigate each of these in turn. The local current density at the plasma edge is driven by bootstrap current, Ohmic current, and a Pfirsch-Schlüter current. The latter parallel current averages out to zero on a flux surface, which allows an easier analysis. Use of the theoretical formulae for the bootstrap current and neoclassical resistivity given by Sauter et al.[6, 7] allows a value of $\langle \boldsymbol{j_{neo}} \cdot \boldsymbol{B} \rangle = \langle \boldsymbol{j_{boot}} \cdot \boldsymbol{B} \rangle + \langle \boldsymbol{j_{Ohmic}} \cdot \boldsymbol{B} \rangle$ to be calculated and compared to $\langle \boldsymbol{j} \cdot \boldsymbol{B} \rangle$ from CLISTE. This is shown in figure 4 for discharge #24681. The large error bars in the CLISTE fit, especially just after the ELM crash, are reflective of the fact that each timepoint is independent of each other one, despite the smooth nature of the timetrace.

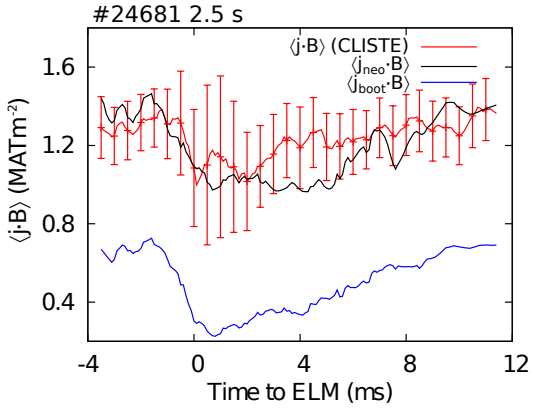

Figure 4: Time traces of $\langle j \cdot B \rangle$ from CLISTE (red), $\langle j_{neo \cdot B} \rangle$ (black), and $\langle j_{boot \cdot B} \rangle$ (blue) over a complete ELM cycle.

The excellent fit of the theoretical calculation to the CLISTE prediction allows analysis of the current density from the point of view of its individual components. The drop in the bootstrap current at the ELM crash is much more than the drop in the CLISTE

predicted $\langle \boldsymbol{j} \cdot \boldsymbol{B} \rangle$; the large drop in non-inductive current is partially compensated by a large increase in the toroidal electric field in the plasma edge. $\langle \boldsymbol{j_{boot}} \cdot \boldsymbol{B} \rangle$ also recovers at a much more gradual pace. This signifies the importance of the Ohmic contribution. The difference that can be seen between 2 and 6 ms in figure 4 is possibly due to different recovery rates of T_i and T_e profiles.

An important addition to this study is an understanding of how the current density scales. Kinetic profiles, created using an mtanh fitting routine, were taken from a large database of ASDEX Upgrade discharges [8] and the magnetic equilibria reconstructed. The resulting 35 individual current density profiles were then tested for scalings based on physical assumptions. One of the most significant findings is a nonlinear dependence of the normalised current density (given by $j = j_{LFS}/\langle j \rangle$) on the pressure gradient, as shown in figure 5.

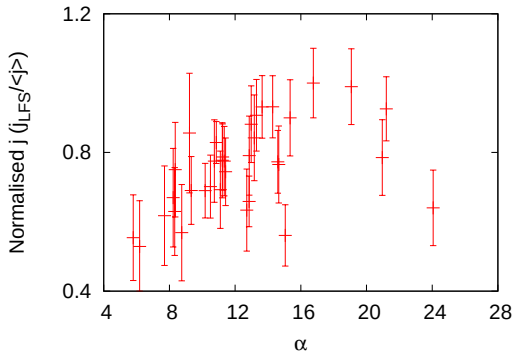

Figure 5: Peak LFS edge current density plotted against normalised pressure gradient for 35 ASDEX Upgrade discharges.

This figure shows a saturation and decline of the current density as we approach higher normalised pressure gradients (defined as $\alpha = -2\mu_0 * \frac{Rq^2}{B_0}\frac{dp}{dr}$). The relevance of this regime to ITER is that the edge current density is responsible for the form of the magnetic shear profile and this can have a stabilising effect on the ballooning mode. If the edge current density were suppressed relative to a linear scaling to a high alpha regime predicted for ITER the form of the edge safety factor would be affected. This would help to stabilise the current driven low-n modes but would also reduce the low shear region.

Acknowledgements

This work was partially supported by EURATOM.

References

[1] A Burckhart et al. *Plasma Physics and Controlled Fusion*, 52(10):105010, October 2010.

[2] D Dickinson et al. *Plasma Physics and Controlled Fusion*, 53(11):115010, November 2011.

[3] M F M De Bock et al. *Plasma Physics and Controlled Fusion*, 54(2):025001, February 2012.

[4] P.J. McCarthy and ASDEX Upgrade Team. *Plasma Physics and Controlled Fusion*, 54(1):015010, January 2012.

[5] M.G. Dunne et al. *Submitted to: Nuclear Fusion*, 2012.

[6] O. Sauter, C. Angioni, and Y. R. Lin-Liu. *Physics of Plasmas*, 6(7):2834, 1999.

[7] O. Sauter, C. Angioni, and Y. R. Lin-Liu. *Physics of Plasmas*, 9(12):5140, 2002.

[8] P.A. Schneider et al. *Submitted to: Plasma Physics and Controlled Fusion*, 2012.